Performance Analysis of OTFS Over Multipath Channels for Visible Light Communication

Anupma Sharma[1], Sandesh Jain[1], Rangeet Mitra[2] and Vimal Bhatia[1] (Senior Member, IEEE)
[1]Discipline of Electrical Engineering, Indian Institute of Technology Indore, India 453552
[1](phd1901202007, phd1601202004, vbhatia)@iiti.ac.in
[2]École de technologie supérieure, University of Quebec, Montreal, Canada, rangeet.mitra.1@ens.etsmtl.ca

***Abstract*—Visible light communication (VLC) is a promising and eco-friendly complementary technology to the existing radio frequency (RF) based communication system. However, the performance of VLC based system is limited by dispersive characteristics of the VLC channel, and restricted modulation bandwidth of light emitting diode (LED). To mitigate the ISI, orthogonal time frequency space (OTFS) modulation is proposed in the literature. However, it has been found that the performance analysis of OTFS over multipath VLC channels has not been investigated. This paper investigates the performance of OTFS over static multipath channels for the VLC system. Simulations performed over the standardized IEEE 802.15.7 VLC channel indicate that OTFS with message passing detector delivers an approximate 6 dB SNR gain at BER of 10^{-4} over the conventional orthogonal frequency division multiplexing (OFDM) scheme with minimum mean square error (MMSE) based detector.**

***Index Terms*—VLC, Message Passing detector, OTFS, OFDM, BER.**

I. Introduction

Visible light communication (VLC) [1] is a green, secure and low-cost complementary technology to the current radio frequency (RF) based communication system. Visible light spectrum offers huge, unregulated and available bandwidth, without electromagnetic interference (EMI) required for the next generation wireless communication system [2]. In VLC, transmission of information symbols is realized via modulating the luminous intensity of a light emitting diode (LED) in accordance to the applied input signal. Widely deployed LEDs play a dual role of illumination and communication. Optical signal received at the receiver is transformed to the electrical domain by the photodiode.

Although promising, performance of a VLC system is limited due to multipaths between receiver and transmitter, which results in inter-symbol-interference (ISI) [3]. Although, many traditional modulation schemes have been implemented in VLC such as pulse position modulation (PPM) [4], on-off keying modulation (OOK) [5], pulse amplitude modulation (PAM) [6]. However, it is difficult to combat ISI due to multipath effects in these modulation schemes, and they also do not support high modulation formats which is not desirable for optimum utilization of available spectrum [7]. To enhance the spectrum, carrier-less amplitude and phase quadrature amplitude modulation (CAP-QAM) scheme is proposed for VLC [8, 9].

To mitigate ISI, various predistorters have been proposed in the literature [3, 10, 11]. Post distortion methods which are complementary to predistorters are also proposed in [12, 13, 14]. To optimize the available spectrum, use of multiplexing technique like optical-orthogonal frequency division multiplexing (O-OFDM) has been proposed in the literature for VLC [15]. Asymmetrically clipped O-OFDM (ACO-OFDM) and DC-biased O-OFDM (DCO-OFDM) are the most noted O-OFDM schemes [16, 17]. However, ACO-OFDM is less spectrally efficient as compared to DCO-OFDM [18]. Although DCO-OFDM provides better spectral gain and lower ISI but receiver complexity increases due to multipath [14]. To mitigate ISI, recently a low complexity generalized orthogonal time frequency space (OTFS) modulation scheme has been proposed in the literature [19, 20, 21].

The OTFS waveform is quasi-periodic which is localized in both time and frequency domain, and hence it is invariant to channel condition [19]. In OTFS, the information symbols are mapped into delay-Doppler domain to resolve the delay and Doppler shift of multipath dynamic wireless channel. These information symbols are then mapped to time-frequency domain similar to OFDM. Due to this mapping, all the transmitted information symbols observe uniform channel gain [19]. In [19], OTFS was compared with traditional OFDM technique with packet error rate (PER) and bit error rate (BER) as the performance analysis metric. In [22], error performance and diversity analysis is performed without biorthogonality assumption. Removing biorthogonality assumption causes extra phase shifts in the transmitted signals and reduces the diversity. In [22], precoding is done to increase diversity. Interference cancellation using OTFS for both rectangular waveforms and ideal pulse waveforms is done in [23]. Novel discrete-time analysis of OFDM-based OTFS transceiver is proposed in [24]. Using single cyclic prefix overhead can be significantly reduced as is done in [25]. In [21], extensive investigation on the performance over static multipath channels is done. In [26], *G.D. Surabhi et. al.* presented a proper analysis of diversity achieved by OTFS modulation. However, the performance of OTFS has been limited for RF and millimeter wave based communication systems. The

978-1-7281-6535-6/20/$31.00 ©2020 IEEE

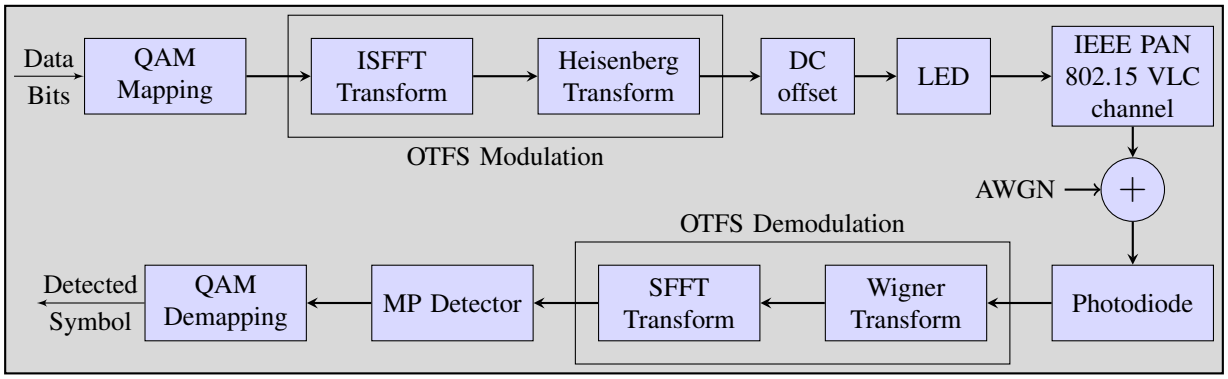

Fig. 1. Block diagram of the considered system model.

performance of a multipath VLC system is limited due to high delay spread [27]. To enhance the performance, OTFS can be used in VLC system for channels with high delay spread [28]. To the best of author's knowledge, and from the literature survey, performance analysis of OTFS is not inquired for VLC.

In this paper, for the first time in the literature, performance of OTFS over static multipath VLC channels is analyzed. Simulations performed over realistic dispersive VLC channel indicate that OTFS gives better BER performance over conventional OFDM scheme. Remainder of the paper is organized as follows: The considered system model is described in Section II. OTFS modulation scheme and message passing (MP) detection algorithm for VLC is described in Section III. Simulation results are given in Section IV. Lastly Section V concludes the paper.

Notations: Scalars, vectors, and matrices are denoted respectively, as a, $\mathbf{a}$, and $\mathbf{A}$. $\mathbf{a}_i$ and $\mathbf{A}_{i,j}$ represent the i^{th} element of vector $\mathbf{a}$ and $(i,j)^{th}$ element of matrix $\mathbf{A}$. The set of matrices with dimension $K \times L$ having each entry from the complex plane is denoted by $\mathbb{C}^{K\times L}$. Let $\mathbf{A} = \text{circ}[\mathbf{A}_0, \ldots, \mathbf{A}_{L-1}] \in \mathbb{C}^{KL\times KL}$ represent the circulant matrix.

II. System Model

Block diagram of the considered system model is given in Fig. 1. Number of symbols and number of sub-carriers are assumed respectively as K and L such that, number of symbols transmitted per frame is N_s equal to KL. Let $\mathbf{x} \in \mathbb{C}^{N_s\times 1}$ be transmitted QAM symbols. First, (2D) inverse symplectic fast Fourier transform (ISFFT) is applied on input QAM modulated vector $\mathbf{x}$ followed by Heisenberg transform on $\mathbf{X}$, where $\mathbf{X}$ is a matrix of dimension $\mathbf{X} \in \mathbb{C}^{K\times L}$ formed by ISFFT of the input vector $\mathbf{x}$.

Before transmission, cyclic prefix (CP) of length $(P-1)$ is appended to the result of Heisenberg transform $\tilde{\mathbf{x}}$, where P is the number of channel paths. After OTFS modulation and adding CP, symbols are transmitted through LED. The output is sent over VLC channel $\mathbf{h}$. Static multipath channel is implied as one with zero Doppler multipaths and P delay multipaths. The channel is represented as $\mathbf{h} = [h_0, h_1, \ldots, h_{P-1}]^T$. The received information signal by the photodiode (after discarding the CP) can be written as

$$\mathbf{r} = \mathbf{H}\tilde{\mathbf{x}} + \mathbf{w} \tag{1}$$

where $\mathbf{H} = \text{circ}[h_0, h_1, \ldots, h_{P-1}, 0, \ldots, 0] \in \mathbb{C}^{N_s\times N_s}$ is the circulant matrix, and $\mathbf{w} \in \mathbb{C}^{N_s\times 1}$ is the additive i.i.d. white Gaussian noise (AWGN) whose i^{th} entry is defined as $w_i \sim \mathcal{CN}(0,\sigma^2)$.

$$\mathbf{H} = \begin{pmatrix} h_0 & h_1 & \cdots & h_{P-1} & \cdots & 0 \\ h_1 & h_2 & \cdots & 0 & \cdots & h_0 \\ \vdots & \vdots & \vdots & \vdots & \vdots & \vdots \\ h_{P-1} & \vdots & \vdots & \vdots & \vdots & \vdots \\ \vdots & 0 & \vdots & \vdots & \vdots & \vdots \\ 0 & h_0 & \cdots & \cdots & \cdots & 0 \end{pmatrix}$$

Similarly, at the receiver, OTFS demodulation is done in two steps. First received symbols are mapped in time-frequency domain using Wigner transform and then to delay-Doppler domain in second step using SFFT. Therefore, the input–output relation of the considered system model in the information domain i.e. delay-Doppler domain can be equated as:

$$\mathbf{y} = \mathbf{H}^{\text{eff}}\mathbf{x} + \tilde{\mathbf{w}} \tag{2}$$

where $\mathbf{y} \in \mathbb{C}^{N_s\times 1}$ is the received symbol in delay-Doppler domain, $\mathbf{H}^{\text{eff}} \in \mathbb{C}^{N_s\times N_s}$ is the effective channel matrix , $\mathbf{x} \in \mathbb{C}^{N_s\times 1}$ is the transmitted QAM symbols and, $\tilde{\mathbf{w}}$ is the noise which has the same statistical properties of $\mathbf{w}$. The received vector $\mathbf{y}$ is passed through MP detector to compute $\hat{\mathbf{x}}$.

III. OTFS with MP detector for VLC

In this Section, OTFS modulation and demodulation scheme employed in the delay-Doppler domain is described. First we will explain the delay-Doppler representation and the various transformations involved. Next, we describe MP detection algorithm in subsection III(A). As given in [19], we can map an arbitrary function in time domain, frequency domain or delay-Doppler domain. These three representation can be interchanged by means of Fourier transform and Zac transform as shown in Fig. 1. Fourier transform can be

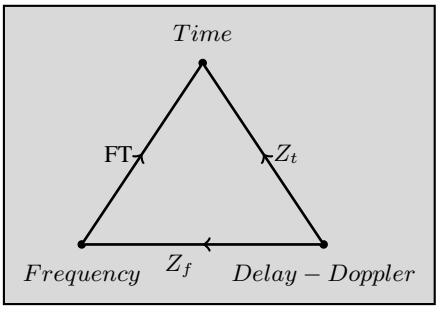

Fig. 2. Transformation triangle

computed with the help of two Zac transforms such that, $FT = Z_t \times Z_f^{-1}$. Signals mapped in the delay-Doppler domain are represented as $\phi(\tau, \upsilon)$, where υ and τ are respectively the variables in Doppler and delay domain. Let τ_r and υ_r denote the delay and Doppler period, such that $\tau_r \upsilon_r = 1$. Thus, conversion from delay-Doppler to time and frequency domain is performed using Zac transforms Z_t and Z_f respectively as [19],

$$\begin{aligned} Z_t(\phi) &= \int_0^{\upsilon_r} e^{j2t\upsilon} \phi(t, \upsilon) d\upsilon, \\ Z_f(\phi) &= \int_0^{\tau_r} e^{-j2\tau f} \phi(\tau, f) d\tau \end{aligned} \tag{3}$$

Instead of using Zac transformation, conversion to time domain from delay-Doppler domain can also be done in a less complex way using the following two steps: (1) delay-Doppler domain to time-frequency domain, (2) time-frequency domain to time domain. The first transformation from delay-Doppler domain to time-frequency domain is realised through 2D ISFFT and the second transformation from time-frequency domain to time domain is through Heisenberg transform.

The channel impulse response in delay-Doppler domain denoted by $\mathbf{h}(\tau, \upsilon)$ is defined as

$$\mathbf{h}(\tau, \upsilon) = \sum_{i=1}^{P} h_i \delta(\tau - \tau_i) \delta(\upsilon - \upsilon_i) \tag{4}$$

where υ_i, τ_i, h_i are Doppler shift, delay and channel gain respectively, for i^{th} cluster and P is the number of channel path. At the transmitter, QAM symbols $\mathbf{x}_{l,k}$ are mapped in delay-Doppler domain. Using ISFFT, these symbols are mapped in the time-frequency domain $\mathbf{X}_{n,m}$, and then using Heisenberg transform to time domain for transmitting $\tilde{\mathbf{x}}(t)$ through LED.

$$\mathbf{X}_{n,m} = \sum_{l=0}^{K-1} \sum_{k=0}^{L-1} \mathbf{x}_{l,k} e^{-j2\pi(\frac{ml}{K} - \frac{nk}{L})} \tag{5}$$

$$\tilde{\mathbf{x}}(t) = \sum_{m=0}^{K-1} \sum_{n=0}^{L-1} \mathbf{X}_{n,m} e^{j2\pi m \Delta f (t - nT)} t_x(t - nT) \tag{6}$$

where $t_x(t)$ is the transmitted pulse. If $t_x(t)$ is a rectangular pulse then Heisenberg transform in (6) reduces to inverse discrete Fourier transform (IDFT). Therefore, the received signal at the photodiode can be written as

$$\mathbf{r}(t) = \int_{\upsilon} \int_{\tau} \mathbf{h}(\tau, \upsilon) \tilde{\mathbf{x}}(t - \tau) e^{j2\pi\upsilon(t-\tau)} d\tau d\upsilon. \tag{7}$$

Similarly, at the receiver, the symbols received in time domain $\mathbf{r}(t)$ are mapped back to time-frequency domain $\mathbf{Y}_{n,m}$ by applying Wigner transform, and then to delay-Doppler domain $\mathbf{y}_{l,k}$ by applying SFFT on $\mathbf{Y}_{n,m}$. Sampling of time-frequency domain is done respectively at intervals T and Δf to obtain a 2D lattice $\Lambda = (nT, m\Delta f)$, where $n = 0, \ldots, L-1$, $m = 0, \ldots, K-1$.

$$\mathbf{Y}_{n,m} = \int \mathbf{r}(\tau) r_x^*(\tau - t) e^{-j2\pi f(t-\tau)} d\tau \tag{8}$$

where r_x is the received pulse. t_x and r_x are ideal pulses i.e. they follows biorthogonality property.

$$\begin{aligned} \mathcal{A}_{r_x, t_x} &= \int t_x(\tau) r_x^*(\tau - t) e^{-j2\pi f(t-\tau)} d\tau \\ \mathcal{A}_{r_x, t_x} &= 0 \end{aligned} \tag{9}$$

$\mathcal{A}_{r_x, t_x}$ is the cross ambiguity function.

$$\mathbf{y}_{l,k} = \frac{1}{\sqrt{KL}} \sum_{n=0}^{L-1} \sum_{m=0}^{K-1} \mathbf{Y}_{n,m} e^{-j2\pi(\frac{ml}{K} - \frac{nk}{L})} \tag{10}$$

In time-frequency domain, input-output relation can be written as

$$\mathbf{Y}_{n,m} = \mathbf{H}_{n,m} \mathbf{X}_{n,m} + \mathbf{W}_{n,m} \tag{11}$$

where $\mathbf{W}_{n,m}$ is AWGN. Channel in time-frequency domain $\mathbf{H}_{n,m}$ is computed as

$$\mathbf{H}_{n,m} = \int_{\tau} \int_{\upsilon} \mathbf{h}(\tau, \upsilon) e^{j2\pi\upsilon nT} e^{-j2\pi(\upsilon + m\Delta f)\tau} d\upsilon d\tau \tag{12}$$

and $\mathbf{X}_{n,m}$ for $n = 0, \ldots, L-1$ and $m = 0, \ldots, K-1$ is the transmitted symbol in a single packet. A single packet is of duration LT and bandwidth of $K\Delta f$. After OTFS demodulation, the information symbols are passed through MP detector for estimating the transmitted symbols and denoted as $\hat{\mathbf{x}}$. The symbols estimated are then compared with the input information symbols $\mathbf{x}$ to calculate BER.

A. Message passing detection algorithm for OTFS

In this Subsection, the MP detection algorithm for VLC is described. The effective channel matrix $\mathbf{H}^{\text{eff}}$ in (2) is sparse [23]. Hence in this paper, MP detection algorithm is implemented in VLC as it has the benefit of inherent channel sparsity [23]. For a channel of P paths, total number of non-zero elements out of N_s in each row and column of $\mathbf{H}^{\text{eff}}$ would be S, where $S < P$. Let $\mathcal{U}_d$ and $\mathcal{V}_c$ be the sets of position of non-zero values, in the d^{th} row and c^{th} column of $\mathbf{H}^{\text{eff}}$, respectively such that $|\mathcal{U}_d| = |\mathcal{V}_c| = S$.

Based on (2), we have modeled our system as a sparse factor graph. There are N_s variable nodes corresponding to $\mathbf{x}$. Similarly, corresponding to $\mathbf{y}$, there are N_s observation nodes. In the factor graph shown in Fig. 3, the observation node $\mathbf{y}_d$ is connected to the set of variable nodes $\{\mathbf{x}_c, c \in \mathcal{U}_d\}$. Similarly,

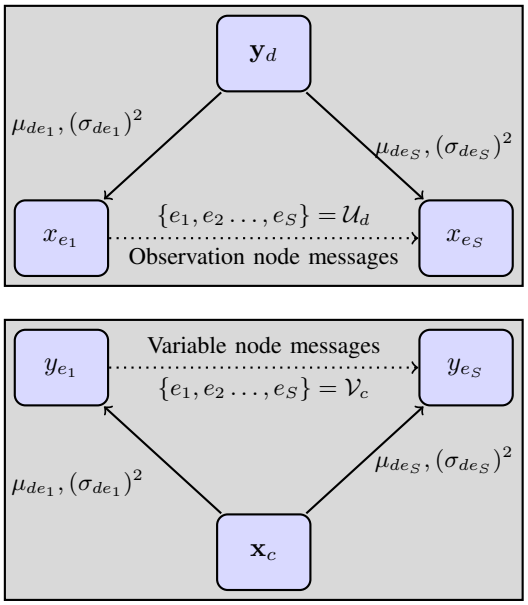

Fig. 3. Messages in factor graph.

Algorithm 1 MP algorithm for detection of OTFS symbols

% ***Input:***
$\mathbf{y}$ (signal vector received) and $\mathbf{H}^{\text{eff}}$ (effective channel matrix)
% ***Initialization:***
Choose probability mass function (pmf) $p_{cd}^{(0)} = \frac{1}{|\mathbb{A}|}$ for $c = \{0, \ldots, N_s - 1\}$ and $d \in \mathcal{V}_c$, $i_{max} = O$
% ***Computation:***
for $i = 1; i < O; i++$

- Compute means $(\mu_{d,c}^{(i)})$ and variances $(\sigma_{d,c}^{(i)})^2$ of interference-plus-noise term $\varrho_{d,c}^{i}$ using $P_{cd}^{(i-1)}$ and pass them through observation nodes to variable nodes as messages.
- Variable node update $P_{cd}^{(i)}$ using the message received and pass it to observation node.
- Update the decision on the information symbol transmitted.
- increment i.

end for
% ***Output:***
$\hat{\mathbf{x}}$ (signal vector detected).

the variable node $\mathbf{x}_c$ is connected to the set of observation nodes $\{\mathbf{y}_d, d \in \mathcal{V}_c\}$.

The joint maximum a posteriori probability (MAP) detection rule for the estimation of the transmitted information symbols from the received symbols is defined as

$$\hat{\mathbf{x}} = \arg \max_{x \in \mathbb{A}^{N_s \times 1}} \Pr(\mathbf{x}|\mathbf{y}, \mathbf{H}^{\text{eff}}), \tag{13}$$

Symbol-by-symbol MAP detection rule is considered for $0 \leq c \leq KL - 1$,

$$\begin{aligned} \hat{\mathbf{x}_c} &= \arg \max_{a_j \in \mathbb{A}} \Pr(\mathbf{x}_c = a_j|\mathbf{y}, \mathbf{H}^{\text{eff}}) \\ &= \arg \max_{a_j \in \mathbb{A}} \frac{1}{|\mathbb{A}|} \Pr(\mathbf{y}|\mathbf{x}_c = a_j, \mathbf{H}^{\text{eff}}) \end{aligned} \tag{14}$$

Assume that, the probability of transmitting all the information symbols $\mathbf{x}_c \in \mathbb{A}$ is same. Also, $\mathbf{y}$ and $\mathbf{x}_c$ are independent of each other due to the sparsity of the channel $\mathbf{H}^{\text{eff}}$.

$$\hat{\mathbf{x}_c} \approx \arg \max_{a_j \in \mathbb{A}} \prod_{e \in \mathcal{V}_c} \Pr(\mathbf{y}_e|\mathbf{x}_c = a_j, \mathbf{H}^{\text{eff}}) \tag{15}$$

In MP, mean and variance of the interference-plus-noise terms (ϱ_{dc}) are transmitted as messages from observation nodes $\mathbf{y}_d$ for $d \in \mathcal{J}_c$ to variable nodes $\mathbf{x}_c$ for each $c = 0, \ldots, N_s - 1$. The probability mass function of the alphabets in $\mathbb{A}$ is defined as:

$$p_{cd} = \{p_{cd}(a_j)|a_j \in \mathbb{A}\} \tag{16}$$

The steps in **Algorithm 1** are detailed below. First initialize the iteration index $i = 1$ and $P_{cd}^0 = \frac{1}{|\mathbb{A}|}$ for $c = \{0, \ldots, N_s - 1\}$ and $d \in \mathcal{V}_c$. Then, messages are passed to the variable nodes $\mathbf{x}_c$ from the observation nodes $\mathbf{y}_d$. Thus, the message passed has a Gaussian probability density function (pdf) which is computed as

$$\begin{aligned} \mathbf{y}_d &= \sum_{e \in \mathcal{U}_d} \mathbf{x}_c (\mathbf{H}^{\text{eff}})_{d,c} + \tilde{\mathbf{w}} \\ &= \mathbf{x}_c (\mathbf{H}^{\text{eff}})_{d,c} + \sum_{e \in \mathcal{U}_d, e \neq c} \mathbf{x}_e (\mathbf{H}^{\text{eff}})_{d,e} + \tilde{\mathbf{w}} \\ &= \mathbf{x}_c (\mathbf{H}^{\text{eff}})_{d,c} + \varrho_{dc} \end{aligned} \tag{17}$$

where ϱ_{dc} is the interference-plus-noise term and $(\mathbf{H}^{\text{eff}})_{d,c}$ is the element in d^{th} row and c^{th} column of $\mathbf{H}^{\text{eff}}$. As the considered noise is Gaussian, ϱ_{dc} can also be approximated as a Gaussian random variable with mean and variance denoted by $\mu_{dc}^{(i)}$, and $(\sigma_{dc}^{(i)})^2$ respectively. The transmitted symbols are presumed to be i.i.d. and independent of noise. Variable nodes send messages to the observation nodes. The new message obtained from $\mathbf{x}_c$ to $\mathbf{y}_d$ carries the pmf vector $P_{cd}^{(i)}$ defined as:

$$P_{cd}^{(i)}(a_j) = \Delta \cdot \hat{P}_{cd}^{(i)}(a_j) + (1 - \Delta) \cdot P_{cd}^{(i-1)}(a_j), \tag{18}$$

where $\Delta \in (0, 1]$ is defined as the damping factor.

$$\hat{P}_{cd}^{(i)}(a_j) \propto \prod_{e \in \mathcal{V}_c, e} \Pr(\mathbf{y_e}|\mathbf{x}_c = a_j, \mathbf{H}^{\text{eff}}), \tag{19}$$

Final decision on the transmitted symbols is thus,

$$\hat{\mathbf{x}}_c = \arg \max_{a_j \in \mathbb{A}} p_c(a_j), \quad c \in \{0, \ldots, KL - 1\} \tag{20}$$

where

$$p_c(a_j) = \prod_{e \in \mathcal{V}_c} (\mathbf{y}_e|\mathbf{x}_c = a_j, \mathbf{H}^{\text{eff}}). \tag{21}$$

IV. SIMULATION RESULTS

In this Section, we provide simulation results to illustrate the performance of OTFS modulation scheme for standardized IEEE 802.15.7 VLC channel models [29]. Three scenarios have been considered in this work: (1) home, (2) open office environment and, (3) open office with cubicles environment as in IEEE 802.15.7 standard. Home environment experiences root mean square (RMS) delay spread and average DC gain of 9.24 ns, and 2.61×10^{-4}, respectively [29]. In open office environment, the RMS delay spread and average DC gain are 15.27 ns, and 8.13×10^{-4}, respectively [29]. For open office with cubicles, RMS delay spread and average DC gain are 12.68 ns, and 7.51×10^{-4} and modulation is done using 16-QAM and 32-QAM. In all the simulations, we have considered $K = 128$ and $N_s = 1024$. At the receiver, low complexity MP detection algorithm is used. It is assumed that perfect channel state information (CSI) is available at the receiver.

TABLE I
SIMULATION PARAMETERS

Parameters	Specifications
Number of symbols transmitted per frame (N_s)	1024
Number of subcarriers (K)	128
Modulation alphabet	16-QAM, 32-QAM

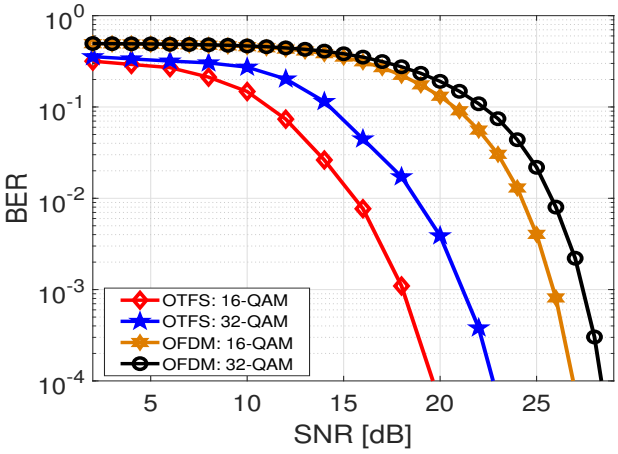

Fig. 4. BER performance of OTFS and OFDM for home environment

Fig. 4 compares the BER performance for OTFS and OFDM for home environment using 16-QAM and 32-QAM. It can be observed from Fig. 4 that OTFS delivers a gain of 6-7 dB at BER of 10^{-4} for both 16-QAM and 32-QAM as all the symbols in OTFS experience uniform channel gain.

The BER performance for OFDM and OTFS for open office environment is shown in Fig. 5 for 16-QAM and 32-QAM. As inferred from Fig. 5, OTFS delivers a gain of 6-7 dB at BER of 10^{-4} for both 16-QAM and 32-QAM as the channel gain is uniform for all the symbols in OTFS.

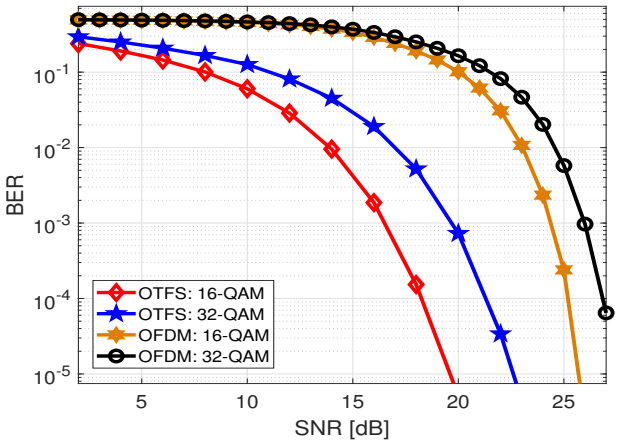

Fig. 5. BER performance of OTFS and OFDM for open office environment

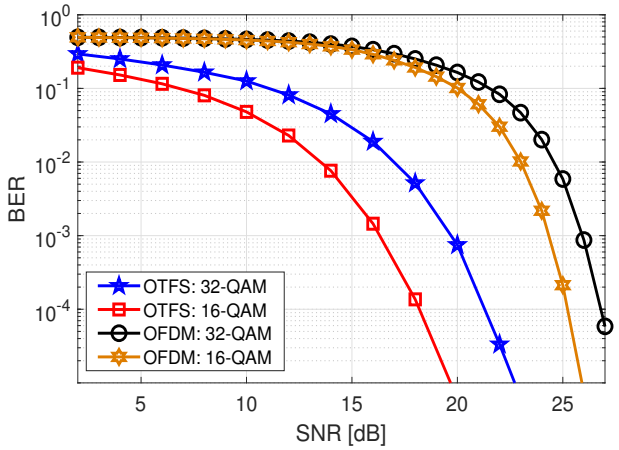

Fig. 6. BER performance of OTFS and OFDM for open office with cubicles environment

In Fig. 6, we present the BER performance for OFDM and OTFS for open office with cubicles environment for 16-QAM and 32-QAM. We observe that, OTFS delivers a gain of 6-7 dB at BER of 10^{-4} for both 16-QAM and 32-QAM. OTFS performs better than OFDM as all the symbols in OTFS experiences uniform channel gain.

V. CONCLUSION

In this paper, the performance analysis of OTFS is explored for visible light communication for static multipath channels. Furthermore, a MP based algorithm is employed for VLC for detection of transmitted symbols. Simulations are performed for standardized IEEE 802.15.7 VLC channel models. Simulations indicates that OTFS with MP detector performs better than OFDM with MMSE detector, which confirms that OTFS is a promising solution for practical deployments of VLC systems for beyond 5G and 6G based communication systems.

VI. Acknowledgment

This publication is an outcome of the R&D work undertaken project under the Visvesvaraya PhD Scheme of Ministry of Electronics & Information Technology, Government of India, being implemented by Digital India Corporation. The authors would also like to thank Indian Institute of Technology Indore for all the support and resources.

References

[1] H. Haas, "LiFi: Conceptions, misconceptions and opportunities," in *2016 IEEE Photonics Conference (IPC)*, Oct 2016, pp. 680–681.

[2] D. C. O'Brien, L. Zeng, H. Le-Minh, G. Faulkner, J. W. Walewski, and S. Randel, "Visible light communications: Challenges and possibilities," in *2008 IEEE 19th International Symposium on Personal, Indoor and Mobile Radio Communications*, Sep. 2008, pp. 1–5.

[3] R. Mitra and V. Bhatia, "Precoding Technique for Ill-Conditioned Massive MIMO-VLC System," in *2018 IEEE 87th Vehicular Technology Conference (VTC Spring)*, June 2018, pp. 1–5.

[4] A. Pradana, N. Ahmadi, T. Adiono, W. A. Cahyadi, and Y. Chung, "VLC physical layer design based on Pulse Position Modulation (PPM) for stable illumination," in *2015 International Symposium on Intelligent Signal Processing and Communication Systems (ISPACS)*, Nov 2015, pp. 368–373.

[5] B. Fahs and M. M. Hella, "3 Gb/s OOK VLC link using bandwidth-enhanced CMOS Avalanche photodiode," in *2017 Optical Fiber Communications Conference and Exhibition (OFC)*, March 2017, pp. 1–3.

[6] L. Grobe and K. Langer, "Block-based PAM with frequency domain equalization in visible light communications," in *2013 IEEE Globecom Workshops (GC Wkshps)*, Dec 2013, pp. 1070–1075.

[7] S. Jain, R. Mitra and V. Bhatia, "On BER analysis of nonlinear VLC systems under ambient light and imperfect/outdated CSI," *OSA Continuum*, vol. 3, no. 11, pp. 3125–3140, Nov 2020.

[8] K. O. Akande, P. A. Haigh, and W. O. Popoola, "On the implementation of carrierless amplitude and phase modulation in visible light communication," *IEEE Access*, vol. 6, pp. 60 532–60 546, 2018.

[9] S. Jain, R. Mitra and V. Bhatia, "Hybrid Adaptive Precoder and Post-Distorter for Massive-MIMO VLC," *IEEE Communications Letters*, vol. 24, no. 1, pp. 150–154, Jan 2020.

[10] R. Mitra and V. Bhatia, "Chebyshev Polynomial-Based Adaptive Predistorter for Nonlinear LED Compensation in VLC," *IEEE Photonics Technology Letters*, vol. 28, no. 10, pp. 1053–1056, May 2016.

[11] S. Jain, R. Mitra and V. Bhatia, "Adaptive Precoding-Based Detection Algorithm for Massive MIMO Visible Light Communication," *IEEE Communications Letters*, vol. 22, no. 9, pp. 1842–1845, 2018.

[12] S. Jain, R. Mitra and V. Bhatia, "Multivariate-KLMS based Post-Distorter for Nonlinear RGB-LEDs for Color-Shift Keying VLC," in *2019 IEEE 30th Annual International Symposium on Personal, Indoor and Mobile Radio Communications (PIMRC)*, 2019, pp. 1–6.

[13] R. Mitra and V. Bhatia, "Unsupervised Multistage-Clustering-Based Hammerstein Postdistortion for VLC," *IEEE Photonics Journal*, vol. 9, no. 1, pp. 1–10, Feb 2017.

[14] R. Mitra, F. Miramirkhani, V. Bhatia and M. Uysal, "Mixture-Kernel Based Post-Distortion in RKHS for Time-Varying VLC Channels," *IEEE Transactions on Vehicular Technology*, vol. 68, no. 2, pp. 1564–1577, Feb 2019.

[15] M. S. A. Mossaad, S. Hranilovic, and L. Lampe, "Visible Light Communications Using OFDM and Multiple LEDs," *IEEE Transactions on Communications*, vol. 63, no. 11, pp. 4304–4313, Nov 2015.

[16] J. Armstrong, "OFDM for Optical Communications," *Journal of Lightwave Technology*, vol. 27, no. 3, pp. 189–204, Feb 2009.

[17] J. B. Carruthers and J. M. Kahn, "Multiple-subcarrier modulation for non-directed wireless infrared communication," in *1994 IEEE GLOBECOM. Communications: The Global Bridge*, vol. 2, Nov 1994, pp. 1055–1059 vol.2.

[18] R. Mesleh, H. Elgala, and H. Haas, "On the Performance of Different OFDM Based Optical Wireless Communication Systems," *IEEE/OSA Journal of Optical Communications and Networking*, vol. 3, no. 8, pp. 620–628, August 2011.

[19] R. Hadani, S. Rakib, M. Tsatsanis, A. Monk, A. J. Goldsmith, A. F. Molisch, and R. Calderbank, "Orthogonal Time Frequency Space Modulation," in *2017 IEEE Wireless Communications and Networking Conference (WCNC)*, March 2017, pp. 1–6.

[20] R. Hadani, S. Rakib, A. F. Molisch, C. Ibars, A. Monk, M. Tsatsanis, J. Delfeld, A. Goldsmith, and R. Calderbank, "Orthogonal Time Frequency Space (OTFS) modulation for millimeter-wave communications systems," in *2017 IEEE MTT-S International Microwave Symposium (IMS)*, June 2017, pp. 681–683.

[21] P. Raviteja, E. Viterbo, and Y. Hong, "OTFS Performance on Static Multipath Channels," *IEEE Wireless Communications Letters*, vol. 8, no. 3, pp. 745–748, June 2019.

[22] E. Biglieri, P. Raviteja, and Y. Hong, "Error Performance of Orthogonal Time Frequency Space (OTFS) Modulation," in *2019 IEEE International Conference on Communications Workshops (ICC Workshops)*, May 2019, pp. 1–6.

[23] P. Raviteja, K. T. Phan, Y. Hong, and E. Viterbo, "Interference Cancellation and Iterative Detection for Orthogonal Time Frequency Space Modulation," *IEEE Transactions on Wireless Communications*, vol. 17, no. 10, pp. 6501–6515, Oct 2018.

[24] A. RezazadehReyhani, A. Farhang, M. Ji, R. R. Chen, and B. Farhang-Boroujeny, "Analysis of Discrete-Time MIMO OFDM-Based Orthogonal Time Frequency Space Modulation," in *2018 IEEE International Conference on Communications (ICC)*, May 2018, pp. 1–6.

[25] P. Raviteja, Y. Hong, E. Viterbo, and E. Biglieri, "Practical Pulse-Shaping Waveforms for Reduced-Cyclic-Prefix OTFS," *IEEE Transactions on Vehicular Technology*, vol. 68, no. 1, pp. 957–961, Jan 2019.

[26] G. D. Surabhi, R. M. Augustine, and A. Chockalingam, "On the Diversity of Uncoded OTFS Modulation in Doubly-Dispersive Channels," *IEEE Transactions on Wireless Communications*, vol. 18, no. 6, pp. 3049–3063, June 2019.

[27] S. Jain, R. Mitra and V. Bhatia, "Kernel MSER-DFE based Post-Distorter for VLC Using Random Fourier Features," *IEEE Transactions on Vehicular Technology*, pp. 1–1, 2020.

[28] S. Jain, R. Mitra and V. Bhatia, "KLMS-DFE based adaptive post-distorter for visible light communication," *Optics Communications*, vol. 451, pp. 353 – 360, 2019.

[29] M. Uysal, F. Miramirkhani, O. Narmanlioglu, T. Baykas, and E. Panayirci, "IEEE 802.15.7r1 Reference Channel Models for Visible Light Communications," *IEEE Communications Magazine*, vol. 55, no. 1, pp. 212–217, January 2017.